Saturable Absorption by Vertically Inserted or Overlaid Monolayer Graphene in Optical Waveguide for All-Optical Switching Circuit

M. Takahashi, Student Member, IEEE
W. Ueda
N. Goto, Member, IEEE
S. Yanagiya, Member, IEEE

Saturable Absorption by Vertically Inserted or Overlaid Monolayer Graphene in Optical Waveguide for All-Optical Switching Circuit
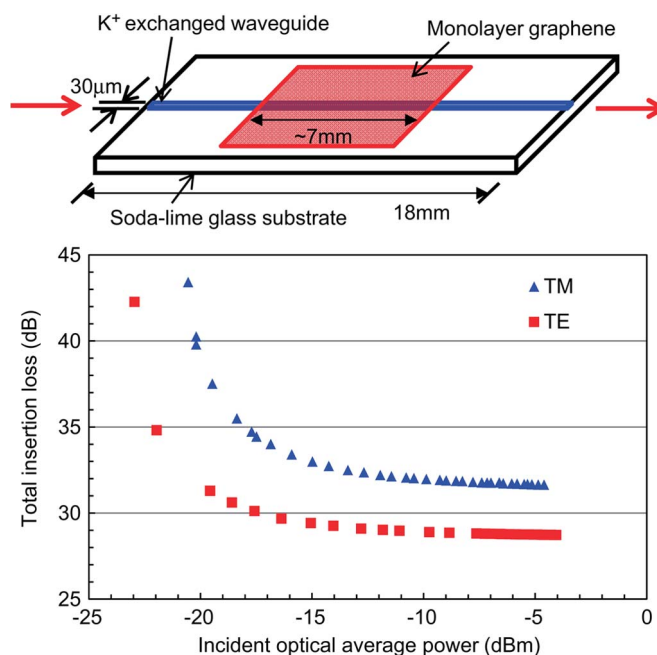
M. Takahashi, *Student Member, IEEE*, W. Ueda, N. Goto, *Member, IEEE*, and S. Yanagiya, *Member, IEEE*

Department of Optical Science and Technology, The University of Tokushima, Tokushima 770-8506, Japan

Abstract: Optical saturable absorption through a monolayer graphene vertically inserted between fibers and overlaid on an ion-exchanged waveguide was measured for picosecond switching application. In our proposed switch, complete switching is performed by controlling the signal light amplitude with the configuration of two cascaded Mach–Zehnder interferometers. To control the signal light amplitude, we use saturable absorption in graphene. For switching, the modulation depth of the amplitude is required to be 2.414, which corresponds to 7.65 dB in intensity. The modulation depth of absorption larger than 10 dB was experimentally obtained in the graphene-loaded waveguide with length of 7 mm.

Index Terms: Optical switch, saturable absorption, graphene.

1. Introduction

Fast-response optical saturable absorption in graphene has been studied to realize short pulse fiber lasers [1], [2], [3]. Optical saturable absorption has been studied using the Z-scan method in monolayer and multiple-layer graphene formed on a sheet of a transparent substrate [4], [5]. Only a few results have been reported on graphene loaded optical planar waveguide. Among them, graphene loaded optical fiber was studied for a TE-pass polarizer [6].

By employing graphene sheets in cascaded interferometers, we proposed a picosecond optical switching device [7]. By controlling signal amplitude, complete switching is performed with the proposed switch architecture. In most of conventional switches, the phase of the optical signal is controlled through refractive-index change. On the contrary, our proposed switch uses a change of the signal amplitude instead of the phase. We proposed to use saturable absorption for controlling the signal amplitude.

In this paper, we briefly describe the theoretical analysis of switching operation in the proposed device. The analytical results are compared with numerical simulation by finite-difference beam-propagation method (FD-BPM). Then, we describe experimental results for optical saturable absorption in monolayer graphene placed vertically in optical fibers with a 1.56 μm femtosecond pulse laser. We also measured saturable absorption through a graphene loaded K$^+$ exchanged waveguide.

We experimentally demonstrated saturable absorption of more than 10 dB modulation depth in a graphene-loaded waveguide. Although the nonlinear absorption was observed using a single light
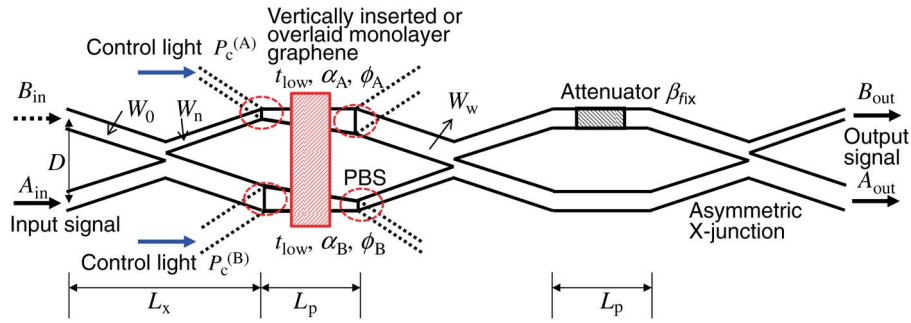
Fig. 1. Switch configuration controlled by saturable absorption in vertically inserted or overlaid graphene on the waveguides.

by varying its intensity, the experimental results proved the feasibility of signal-light control by an intense control light, which is required in the proposed switch.

2. Optical Switch Configuration and Conditions Required for Switching

Fig. 1 shows the proposed switch architecture consisting of two Mach-Zehnder interferometers (MZIs) connected with three asymmetric X-junction couplers. Switching can be operated by controlling the amplitude of the incident signal light. In our first proposed device, optical Raman amplifiers were employed to control the signal light, where multiple-wavelength signals can be independently controlled by wavelength multiplexed control light [8]. Similar switching can be realized by controlling absorption for signal light. Although wavelength-independent controllability cannot be realized, simple device structure can be adopted. The proposed device shown in Fig. 1 employs a single sheet of monolayer graphene loaded on the optical waveguides in the first MZI. An alternative to introduce graphene in the waveguide is to insert multiple sheets of graphene vertically at the cross-section of the two arms. The absorption in the graphene-introduced waveguide is controlled by the intense control light whose polarization or wavelength differs from that of signal light. Optical input and output waveguides for control light are shown in dotted lines. Polarization selective couplers or wavelength selective couplers are used as the combining or separating branches denoted by dashed ellipses. PBS denotes a polarization beam splitter used for polarization selective coupling.

We consider a model for controlling the transmittance through a graphene-introduced waveguide. The signal light with electrical-field amplitude $P_{s,in}$ attenuates to be $P_{s,out}$ through the vertically inserted graphene sheets or the graphene loaded waveguide, as shown in Fig. 2(a) or (b), respectively. The intense control light with electrical-field amplitude $P_{c,in}$ also attenuates to be $P_{c,out}$. The attenuation of the signal light can be decreased by the intense control light due to saturable absorption of graphene. This control of absorption can be equivalently represented by a cascade connection of a fixed attenuator with amplitude attenuation coefficient t_{low} and an amplifier controlled by the control light whose amplitude amplification coefficient is α. The amplification corresponds to decrease of the absorption due to the saturable absorption induced by the intense control light. These coefficients are defined by

$$t_{low} = \frac{P_{s,out}(P_{c,in} = 0)}{P_{s,in}}, \qquad (1)$$

$$\alpha = \frac{P_{s,out}(P_{c,in} \neq 0)}{P_{s,out}(P_{c,in} = 0)}. \qquad (2)$$

Since nonlinear absorption is accompanied by phase shift ϕ, we define α' by

$$\alpha' = \alpha e^{j\phi}. \qquad (3)$$

The transmission of the graphene inserted or loaded waveguide in arm A or B can be modeled by an attenuator having amplitude attenuation coefficient t_{low}, an amplifier having amplitude
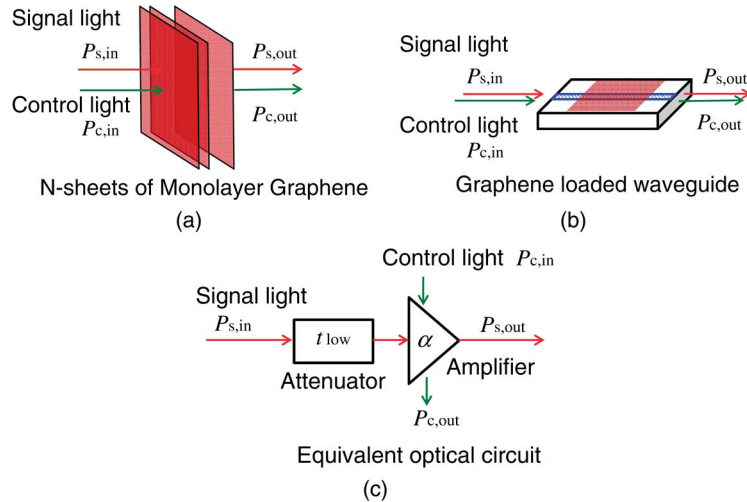
Fig. 2. Model of optical signal light controlled by control light through saturable absorption; (a) the signal and control lights are vertically incident in the multiple sheets of graphene, (b) the signal light is controlled through graphene loaded waveguide, and (c) an equivalent model with a fixed attenuator and an amplifier for signal light.

amplification coefficient of α_i, and phase shift ϕ_i, $i = A$ or B, respectively. A fixed attenuator with amplitude attenuation coefficient β_{fix} is employed in one arm of the second MZI.

The output fields A_{out} and B_{out} of the switch shown in Fig. 1 are related to the input fields A_{in} and B_{in} as

$$
\begin{aligned}
\begin{pmatrix} A_{out} \\ B_{out} \end{pmatrix} &= \left(\frac{1}{\sqrt{2}}\right)^3 \begin{pmatrix} 1 & 1 \\ -1 & 1 \end{pmatrix} \begin{pmatrix} 1 & 0 \\ 0 & \beta_{fix} \end{pmatrix} \begin{pmatrix} 1 & 1 \\ -1 & 1 \end{pmatrix} \begin{pmatrix} t_{low}\alpha'_B & 0 \\ 0 & t_{low}\alpha'_A \end{pmatrix} \begin{pmatrix} 1 & 1 \\ -1 & 1 \end{pmatrix} \begin{pmatrix} A_{in} \\ B_{in} \end{pmatrix} \\
&= \frac{t_{low}}{2\sqrt{2}} \begin{pmatrix} a_{11} & a_{12} \\ a_{21} & a_{22} \end{pmatrix} \begin{pmatrix} A_{in} \\ B_{in} \end{pmatrix},
\end{aligned} \tag{4}
$$

where

$$
\begin{cases}
a_{11} = -\alpha'_A + \alpha'_B - \beta_{fix}(\alpha'_A + \alpha'_B) \\
a_{12} = \alpha'_A + \alpha'_B + \beta_{fix}(\alpha'_A - \alpha'_B) \\
a_{21} = \alpha'_A - \alpha'_B - \beta_{fix}(\alpha'_A + \alpha'_B) \\
a_{22} = -\alpha'_A - \alpha'_B + \beta_{fix}(\alpha'_A - \alpha'_B).
\end{cases} \tag{5}
$$

When optical signal is incident only at one input port as $A_{in} = E_{in}$ and $B_{in} = 0$, Eq. (4) becomes

$$
\begin{pmatrix} A_{out} \\ B_{out} \end{pmatrix} = \frac{t_{low}E_{in}}{2\sqrt{2}} \begin{pmatrix} a_{11} \\ a_{21} \end{pmatrix}. \tag{6}
$$

From this equation, we find the conditions for switching as follows:

i) When $\alpha_A = 1 + \sqrt{2}$, $\alpha_B = 1$, $\phi_A = 2m\pi$, $\phi_B = 0$, and $\beta_{fix} = 1/(1 + \sqrt{2})$,

$$
\begin{pmatrix} A_{out} \\ B_{out} \end{pmatrix} = -t_{low}E_{in} \begin{pmatrix} 1 \\ 0 \end{pmatrix}. \tag{7}
$$

ii) When $\alpha_A = 1$, $\alpha_B = 1 + \sqrt{2}$, $\phi_A = 0$, $\phi_B = 2m\pi$, and $\beta_{fix} = 1/(1 + \sqrt{2})$,

$$
\begin{pmatrix} A_{out} \\ B_{out} \end{pmatrix} = -t_{low}E_{in} \begin{pmatrix} 0 \\ 1 \end{pmatrix}, \tag{8}
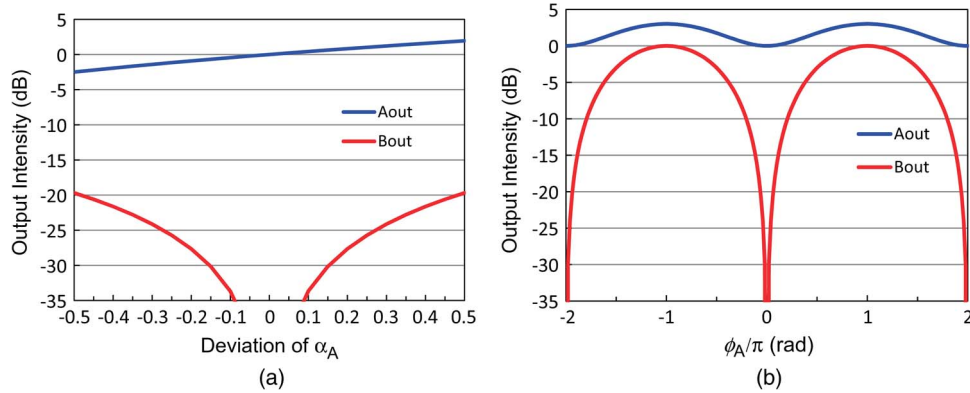$$

Fig. 3. Degradation of switching performance; (a) output intensities as a function of deviation of α_A from $\alpha_A = 1 + \sqrt{2}$, and (b) output intensities as a function of phase shift ϕ_A.

where $m = 0, 1, 2, \ldots$. Therefore, amplification of the amplitude coefficient of $1 + \sqrt{2} \simeq 2.414$ is required for switching. It is noted that switching to A_{out} or B_{out} is operated by increasing either α_A or α_B by adding control light either in the upper arm or in the lower arm of the first MZI, respectively. The operation principle was discussed in detail in ref. [7]. This proposed switch can be operated over a wide wavelength range because the saturable absorption in graphene is observed in a wide wavelength range [5] in addition to the wavelength insensitive configuration of the proposed device [8]. This amplification coefficient corresponds to the value $(1 + \sqrt{2})^2 \simeq 5.827$ (7.65 dB) for light intensity. Since the switch consists of attenuators alone, inevitable attenuation of t_{low}^2 for the signal intensity is accompanied. The value of attenuation depends on the optical waveguide structure and the overlaid graphene length.

Fig. 3(a) shows the output intensities as a function of a deviation $\Delta\alpha_A$ of α_A from $\alpha_A = 1 + \sqrt{2}$, where $\alpha_B = 1$ and $\phi_A = \phi_B = 0$. The extinction ratio of switching is larger than 25 dB for $-0.24 < \Delta\alpha_A < 0.31$. On the other hand, the output intensities depend on a phase shift ϕ_A, as shown in Fig. 3(b). It is found that complete switching is operated at $\phi_A = 0, \pm 2\pi$. The phase shift has to be smaller than $-0.06 < \phi_A/\pi < 0.06$ to keep the extinction ratio larger than 20 dB. It was reported that the propagation constant changes due to saturable absorption in graphene [9], [10]. Therefore, for switching, the phase shift ϕ_i has to be adjusted to zero or an integer multiple of 2π. This condition can be satisfied by designing the length of the graphene loaded region and the control light intensity because the absorption and the phase shift are expected to have different dependence on light intensity [10]. Even for the vertically inserted graphene, phase shift is accompanied [10]. More detail investigation is indispensable to operate the switch more effectively.

If the phase change is large enough compared with the absorption change, a single MZI with graphene sheets in each arm can be an alternative switch configuration as a similar manner with electrically controlled switches or modulators. However, if the nonlinear absorption cannot be negligible, switching becomes incomplete.

3. FD-BPM Simulation of Switching

The switching operation is numerically simulated by FD-BPM. We consider a two-dimensional slab waveguide model. The core and cladding regions have refractive indexes of $n_c = 1.461$ and $n_s = 1.45$, respectively. The waveguide widths of the fundamental, narrow, and wide waveguides of the asymmetric X-junctions are $W_1 = 3.0~\mu m$, $W_n = 2.6~\mu m$, and $W_w = 3.4~\mu m$, respectively. Optical waves are assumed to be TE mode. The lengths of the X-junction coupler and the parallel waveguides are $L_x = 16$ mm and $L_p = 1$ mm, respectively. The total length is 50 mm. The distance of the input ports is $D = 23~\mu m$.

The switching operation at $\lambda = 1550$ nm is confirmed, as shown in Fig. 4, where squared electric fields $|E|^2$ are plotted. In the simulation, amplification is equivalently simulated just by increasing the
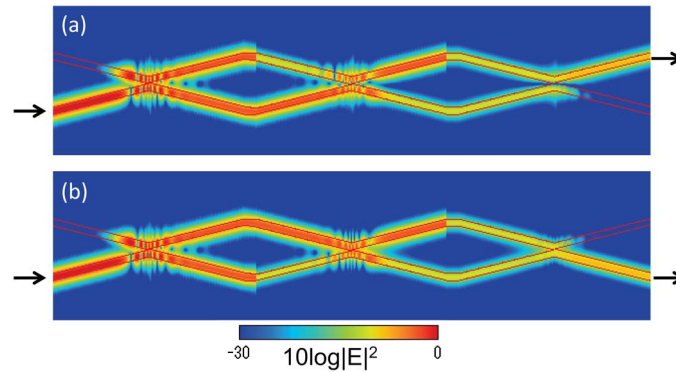
Fig. 4. BPM simulation results of switching operation with (a) $\alpha_A = 1$, $\alpha_B = 1 + \sqrt{2}$ and (b) $\alpha_A = 1 + \sqrt{2}$, $\alpha_B = 1$.

TABLE 1

Comparison of optical output intensities between theoretical analysis and simulation

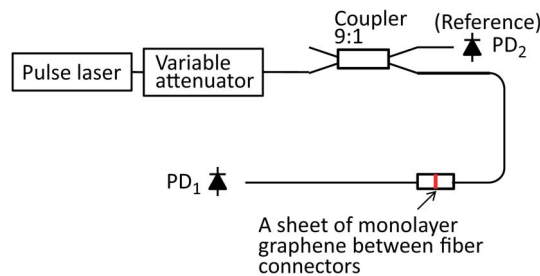| Control	Theory		Simulation	
	$|A_{out}|^2$	$|B_{out}|^2$	$|A_{out}|^2$	$|B_{out}|^2$
Arm B	0	0.1716	6.281×10^{-4}	1.653×10^{-1}
Arm A	0.1716	0	1.689×10^{-1}	6.195×10^{-4}

Fig. 5. Experimental setup for nonlinear transmittance through graphene between fibers.

electric field by multiplying the coefficient α_i at a plane located at the end of the graphene-loaded or inserted waveguide. No phase shift ϕ_i is assumed in this simulation. The waveguides for coupling the control light are not modeled in this simulation. In a similar manner, the attenuator is modeled by multiplying the electric field by t_{low} or β_{fix}. The value of t_{low} is assumed to be an ideal value of $1/(1 + \sqrt{2})$, where the optical signal does not attenuate through graphene with intense control light. It is found from this simulation result that the switching is successfully operated. The normalized output intensities are summarized in Table 1. Good agreement was obtained between the theoretical result and the simulated one.

4. Measurement of Saturable Absorption

4.1. Vertically Inserted Graphene Between Fibers

Instead of vertically inserting graphene sheets in the optical waveguides, a single sheet of monolayer graphene transferred on an end facet of a fiber connector was used to measure nonlinear transmittance. The experimental setup for measuring nonlinear absorption is shown in Fig. 5. A 1.56 μm femtosecond laser with width of 0.4 ps at repetition rate of 41.96 MHz was used as the laser source. The average power is 4.4 mW. The lasing spectrum is shown in Fig. 6.
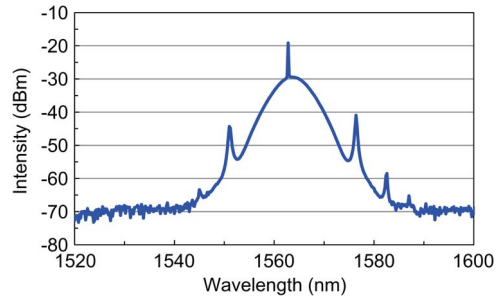
Fig. 6. Spectrum of lasing output from the femtosecond laser.
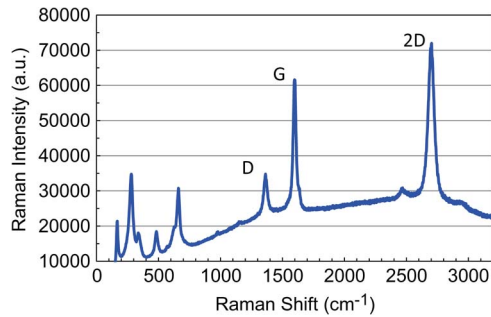

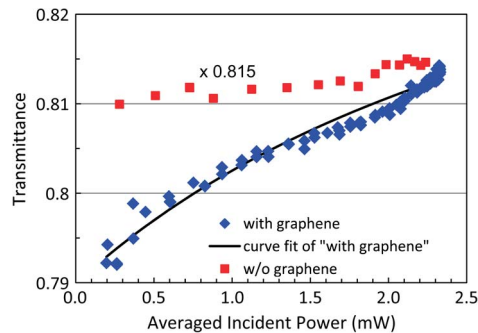Fig. 7. Raman spectrum from a sheet of graphene on a fiber end.

Fig. 8. Transmittance through graphene transferred on a fiber end facet.

A sheet of monolayer graphene formed by CVD on copper foil (iTRIX Corporation) was transferred on the fiber end facet. The Raman spectrum for a single graphene transferred on the fiber end is shown in Fig. 7. This spectrum was measured at the graphene just beside the fiber instead on the fiber cross-section to avoid nonlinear scattering along the fiber. It is found from the measured Raman peaks that a monolayer graphene is successfully transferred on the fiber end facet. Transmittance as a function of incident optical power is shown in Fig. 8, where the transmittance through a fiber without graphene is also plotted. A fitted curve for the transmission $T(I)$ with the graphene film given by the following equation is also plotted, where I is the optical incident power:

$$T(I) = 1 - \left[\frac{\alpha_0}{1 + I/I_{sat}} + \alpha_{ns} \right], \tag{9}$$

where I_{sat} is the saturation intensity, α_0 is the modulation depth, and α_{ns} is the non-saturable loss. These parameters for the fitted curve are $I_{sat} = 3.6$ mW, $\alpha_0 = 0.058$, and $\alpha_{ns} = 0.152$. The increase of transmittance through a single sheet of graphene is about 2%. Note that the transmittance
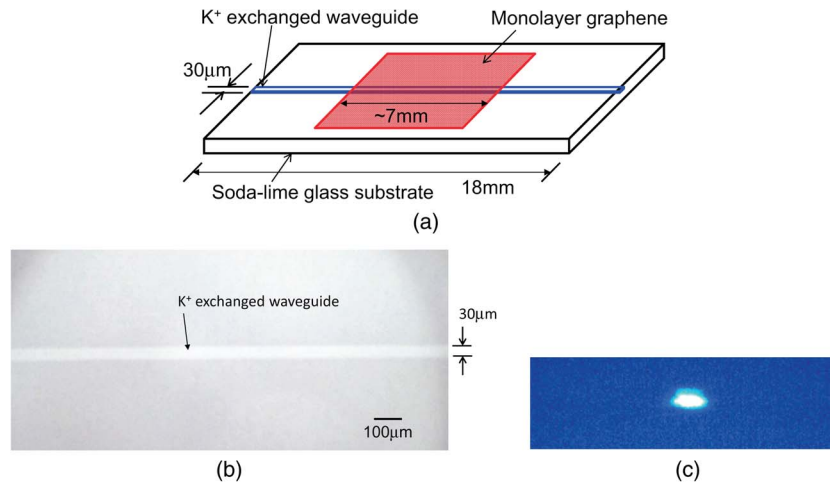
Fig. 9. (a) Waveguide structure with overlaid graphene sheet, (b) the microscopic top-view picture, and (c) an output near field pattern.
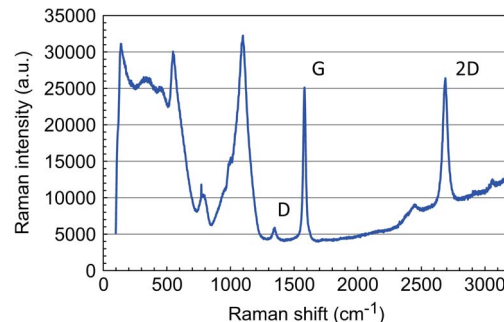

Fig. 10. Raman spectrum of graphene loaded waveguide.

change through a single monolayer graphene was reported to be around 2.3% [1]. Although the change of the transmittance due to increase of the optical power is not sufficient for application to optical switch shown in Fig. 1, increasing the incident optical power and increasing the number of the multiple graphene sheets are considered to satisfy the requirement for switching.

4.2. Loaded Graphene on Ion-Exchanged Waveguide

Next, we measured optical saturable absorption in a monolayer-graphene-loaded waveguide. The optical waveguide was fabricated by K^+ ion exchange on a soda-lime glass substrate. Optical channel waveguide was formed by ion exchange through a 30 μm opening in an aluminum mask. Potassium nitrate was used as the ion source, and ion exchange was carried out at 370 °C for 4 h. The refractive index of the substrate is approximately 1.507 at $\lambda = 1.55$ μm, and the index increase by K^+ ion exchange is around 1×10^{-2} [11], [12].

After polishing both end facets of the waveguide, a sheet of monolayer graphene was transferred on the glass substrate surface. The length of the graphene sheet is about 7 mm. The waveguide structure is shown in Fig. 9(a). The microscopic picture of the surface is shown in (b). A measured near field pattern at the waveguide output for $\lambda = 1.56$ μm is shown in (c). Raman spectrum of the transferred graphene on the glass substrate was measured, as shown in Fig. 10. It is found from the measured Raman peaks that a monolayer graphene is successfully transferred on the substrate.

The experimental setup for measuring saturable absorption is illustrated in Fig. 11. A 1.56 μm femtosecond laser was used as the laser source. The polarization-controlled laser light was coupled into the waveguide by ×20 objective lens.
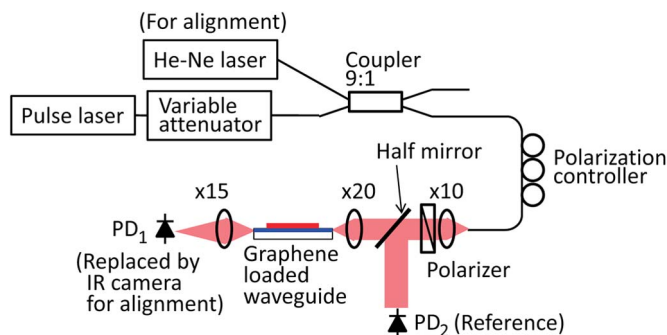
Fig. 11. Experimental setup for measuring nonlinear absorption through a graphene loaded waveguide.
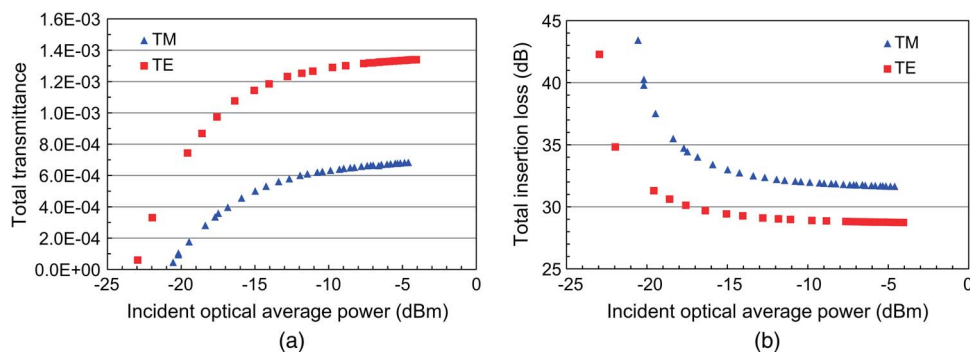

Fig. 12. Measured saturable absorption; (a) total transmittance and (b) total insertion loss.

Fig. 12(a) shows the measured transmittance for TE and TM modes as a function of the incident average power at the waveguide input. The transmittance includes coupling loss, waveguide-propagation loss, and attenuation loss due to graphene. The calculated loss in decibel is also shown in (b). The insertion loss reduces by more than 10 dB as the incident power increases. This is considered to be caused by saturable absorption of graphene. This modulation depth of the transmittance through the waveguide satisfies the requirement for optical switching. The insertion loss in TM mode is larger than that in TE mode by about 10 dB at low optical power. The difference reduces to about 3 dB at high optical power.

5. Conclusion

An optical switch controlled by saturable absorption of graphene vertically inserted or loaded on the waveguide was proposed. Preliminary experiments on saturable absorption through a graphene inserted fiber and a graphene-loaded waveguide show that the measured modulation depth of the absorption can meet the requirement for switching.

Although the incident light intensity was changed in the preliminary experiments, a weak signal light has to be controlled by an intense control light in the proposed switch. We will investigate signal light control by orthogonally polarized control light or by different-wavelength control light. Experimental verification of switching will be investigated in the future.

References

[1] S. Yamashita, "A tutorial on nonlinear photonics applications of carbon nanotube and graphene," *J. Lightwave Technol.*, vol. 30, no. 4, pp. 427–447, Feb. 2012.
[2] Q. Bao, H. Zhang, Y. Wang, Z. Ni, Y. Wang, Z. X. Shen, K. P. Loh, and D. Y. Yang, "Atomic-layer graphene as a saturable absorber for ultrafast pulsed lasers," *Adv. Funct. Mater.*, vol. 19, no. 19, pp. 3077–3083, Oct. 2009.

[3] Z. Sun, T. Hasan, F. Torrisi, D. Popa, G. Privitera, F. Wang, F. Bonaccorso, D. M. Basko, and A. C. Ferrari, "Graphene mode-locked ultrafast laser," *ACS Nano*, vol. 4, no. 2, pp. 803–810, 2010.

[4] Q. Bao, H. Zhang, Z. Ni, Y. Wang, L. Polavarapu, Z. Shen, Q. H. Xu, D. Tang, and K. P. Loh, "Monolayer graphene as a saturable absorber in a mode-locked laser," *Nano Res.*, vol. 4, no. 3, pp. 297–307, Mar. 2011.

[5] Z. Zheng, C. Zhao, S. Lu, Y. Chen, Y. Li, H. Zhang, and S. Wen, "Microwave and optical saturable absorption in graphene," *Opt. Exp.*, vol. 20, no. 21, pp. 23 201–23 214, Oct. 2012.

[6] Q. Bao, H. Zhang, B. Wang, Z. Ni, C. Haley, Y. X. Lim, Y. Wang, D. Y. Tang, and K. P. Loh, "Broadband graphene polarizer," *Nature Photon.*, vol. 5, no. 7, pp. 411–415, Jul. 2011.

[7] M. Oya, H. Kishikawa, N. Goto, and S. Yanagiya, "All-optical switch consisting of two-stage interferometers controlled by using saturable absorption of monolayer graphene," *Opt. Exp.*, vol. 20, no. 24, pp. 27 322–27 330, Nov. 2012.

[8] H. Kishikawa, K. Kimiya, N. Goto, and S. Yanagiya, "All-optical wavelength-selective switch consisting of asymmetric X-junction couplers and Raman amplifiers for wide wavelength range," *IEEE/OSA J. Lightwave Technol.*, vol. 28, no. 1, pp. 172–180, Jan. 2010.

[9] A. Auditore, C. De Angelis, A. Locatelli, S. Boscolo, M. Midrio, M. Romagnoli, A.-D. Capobianco, and G. Nalesso, "Graphene sustained nonlinear modes in dielectric waveguides," *Opt. Lett.*, vol. 38, no. 5, pp. 631–633, Mar. 2013.

[10] H. Zhang, S. Virally, Q. Bao, L. K. Ping, S. Massar, N. Godbout, and P. Kockaert, "Z-scan measurement of the nonlinear refractive index of graphene," *Opt. Lett.*, vol. 37, no. 11, pp. 1856–1858, Jun. 2012.

[11] M. Rubin, "Optical properties of soda lime silica glasses," *Solar Energy Mater.*, vol. 12, no. 4, pp. 275–288, Sep./Oct. 1985.

[12] G. L. Yip and J. Albert, "Characterization of planar optical waveguides by K$^+$-ion exchange in glass," *Opt. Lett.*, vol. 10, no. 3, pp. 151–153, Mar. 1985.